I&EC research
Industrial & Engineering Chemistry Research

Article

pubs.acs.org/IECR

Dependence of Steady-State Compositional Mixing Degree on Feeding Conditions in Two-Component Aggregation

Haibo Zhao*[,†] and Frank Einar Kruis[‡]

[†]State Key Laboratory of Coal Combustion, Huazhong University of Science and Technology, Wuhan, 430074 P. R. China

[‡]Institute of Technology for Nanostructures (NST) and Center for Nanointegration Duisburg-Essen (CENIDE), University of Duisburg-Essen, Duisburg, 47057 Germany

ABSTRACT: Two-component aggregative mixing of initially bidisperse particle populations results in a Gaussian-type compositional distribution function, which can be fully described by the overall mass fraction of component A (ϕ) and the mass-normalized power density of excess component A (χ, indicating the mixing degree). χ will reach a steady-state value once the self-preserving size distribution is attained. The relation between the steady-state value of χ (χ_∞) and its initial value (χ_0) has not been investigated before. This paper applies population balance modeling to gain insight into the dependence of χ_∞ on initial feeding conditions. By model fitting from hundreds of systematically varied simulations, it is found that χ_∞/χ_0, which depends on ϕ, can be formalized by the Gaussian-type function for Brownian aggregation in the free-molecular regime as well as in the continuum regime, however with different geometric standard deviations. The present work can help to optimize mixing by properly selecting the initial mass and number concentrations of components A and B in the feed.

INTRODUCTION

In particulate processing, the relevant particles properties such as volume, surface area, charge, and composition are usually distributed properties. The particle number balance (which is formally referred to as the population balance) can be formulated by an extension of the continuous Smoluchowski equation, representing the temporal evolution of distribution functions of multiple internal variables (multivariate population balance). It can take into account dynamic events such as coagulation, breakage, nucleation, surface growth, dissolution or evaporation and deposition.[1] Multivariate population balance modeling (PBM), which is relevant for, e.g., combustion-synthesized nanoparticles[2] and atmospheric aerosols,[3] is a very challenging task. This is due to the complicated kinetic functions as well as the difficulties in solving the partial integro-differential population balance equation (PBE). An important type of multivariate PBM is multicomponent aggregation, describing the formation of larger particles caused by binary collisions of particles having different chemical components. Synonyms such as coagulation, agglomeration, and coalescence are also used in different fields of science.

In many processes (including polymerization,[4] wet granulation,[5] crystallization,[6] atmospheric aerosols,[7] and nanoparticle synthesis[8]), aggregation represents the most ubiquitous physical mechanism of size enlargement. Since the aggregating particles are often inhomogeneous in chemical composition, even in nonreactive systems, the compositional distribution undergoes a dynamic evolution. The relevant properties of particles are usually influenced by their compositional distribution. For example, thin films of FePt nanoparticles are among the most promising candidates for magnetic information storage. In high-temperature gas-phase synthesis of FePt nanoparticles it is important that the $L1_0$ crystal phase is formed, as it shows hard-magnetic properties. However, this phase can only be formed when between 40 and 60 mol % Pt is present in the nanoparticles.[9] Thus, describing the evolution of the compositional distribution is necessary to optimize the particle synthesis process. In this paper, we consider two-component aggregative mixing, starting from primary particles containing either component A or component B which then aggregate into larger particles which do not react chemically.

In two-component aggregative mixing, the focus is on the evolution of the compositional distribution and the degree of mixing. Furthermore, it is relevant to know how to obtain a certain level of mixing by modifying initial conditions such as number concentration and volume of the primary particles. There are a limited number of studies dealing with theoretical analysis of two-component aggregation. Krapivsky and Ben-Naim developed a two-parameter scaling law for analytical solution of two-component aggregation with a constant kernel, which is characterized by Gaussian statistics.[10] Vigil and Ziff further extended this scaling theory to nonconstant kernels that may be composition-dependent or -independent and showed that the compositional distribution within each size class is a Gaussian function, irrespective of the kernel and the initial conditions.[11] An initially bidisperse and two-component population can be expressed in terms of initial number concentration N_{A0} and initial particle mass m_{A0} for component A as well as related ones for component B. The compositional distribution of component A is denoted by the probability density function $g(m_A|m)dm_A$ which is the fraction of particles of mass m that contains component A in the mass amount (m_A, m_A+dm_A). This probability density $g(m_A|m)$ was found to be a Gaussian function from the random-mixing theory and the central-limit theorem,[12−14] as well as from PBM using Monte

Received: January 23, 2014
Revised: March 20, 2014
Accepted: March 20, 2014
Published: March 20, 2014

   dx.doi.org/10.1021/ie500316g | Ind. Eng. Chem. Res. 2014, 53, 6047−6055

Carlo techniques based on the constant-number method and the differentially weighted Monte Carlo method:[13,15]

$$g(m_A|m,\,t) = \frac{1}{\sqrt{2\pi m\chi}}\exp\left[-\frac{(m_A - \phi m)^2}{2m\chi}\right] \tag{1}$$

where ϕ is the overall mass fraction of component A

$$\phi = \frac{M_A}{M_A + M_B} \tag{2}$$

and $M_A = N_{A0}m_{A0}$ is the initial mass concentration of component A. ϕ does not change during the aggregative mixing process. The degree of mixing in the population is quantified by χ, which is the mass-normalized power density of excess component A, defined as[12]

$$\begin{aligned}\chi &= \frac{X^2}{M}\\ &= \frac{\int_0^\infty dm_A\int_0^\infty dm_B x^2 n(m_A,\,m_B,\,t)}{\int_0^\infty dm_A\int_0^\infty dm_B(m_A + m_B)n(m_A,\,m_B,\,t)}\\ &= \frac{\int_0^\infty dm\int_0^m dm_A x^2 f(m,\,t)g(m_A|m,\,t)}{\int_0^\infty dm\int_0^m dm_A m f(m,\,t)g(m_A|m,\,t)}\end{aligned} \tag{3}$$

where X^2 is the sum-square (or total variance) of excess component A (x), representing a single-point measure of the degree of mixing between the two components;[12] M is the total mass of particles ($=M_A + M_B$), i.e., the first-order moment of $n(m_A,m_B,t)$ in m; $n(m_A,m_B,t)$ is the number density function at time t and $n(m_A,m_B,t)dm_Adm_B$ represents the number concentration of particles in the mass range of component A, m_A to $m_A + dm_A$, and the mass range of component B, m_B to $m_B + dm_B$; $f(m,t)$ is the component-independent particle size distribution function such that $f(m,t)\,dm$ represents the number concentration of particles in the mass range of m to $m + dm$; x is the amount of component A in excess of the amount ϕm

$$x = m_A - \phi m = m_A - \phi(m_A + m_B) \tag{4}$$

The smaller χ is, the better the mixing of the two components. More recently, Matsoukas and his co-workers found from mean-field PBEs that χ always reaches a steady-state value for two-component aggregation with composition-independent or -dependent kernels.[12−14] It was also found that the compositional distributions become self-preserving, similar to particle size distributions in monocomponent systems[15,16] and that the self-preserving state is reached when the degree of mixing (χ) reaches its steady-state value. Therefore, provided that the steady-state value of χ (χ_∞) is known in advance, the compositional distribution in the size interval $\langle m_{sp}^-,\,m_{sp}^+\rangle$ is given by

$$g(m_A|m,\,t) = \frac{1}{(m_{sp}^+ - m_{sp}^-)}\int_{m_{sp}^-}^{m_{sp}^+}\frac{1}{\sqrt{2\pi m\chi_\infty}}\exp\left[-\frac{(m_A - \phi m)^2}{2m\chi_\infty}\right]dm_A \tag{5}$$

Matsoukas et al. concluded that χ_∞ is the single most important parameter controlling the degree of mixing between components and that it is largely controlled by the initial state.[13] In other words, it is possible to optimize mixing by properly selecting the initial mass and number concentrations of component A and B in the feeding. However, the steady-state value χ_∞ is not exactly known. The aim of this paper is to gain insight into the relation between χ_∞ and the initial value χ_0 (here $\chi_0 = (1 - \phi)\phi(m_{A0}(1 - \phi) + m_{B0}\phi)$) in two-component aggregation processes.

The remainder of this paper is organized as follows. First, the differentially weighted Monte Carlo (DWMC) method for two-component PBM is briefly introduced.[15,17] An accelerated version of the DWMC method is adopted here in combination with a composition-dependent shift action which distributes a limited number of simulation particles as homogeneously as possible over the compositional space. Then, the numerical results for composition-independent as well as composition-dependent aggregative mixing are shown. By varying the initial conditions, the possible influencing factors on χ_∞/χ_0 are analyzed and an empirical formula giving an estimation of χ_∞/χ_0 is found. In the next section the application of the proposed formula to predict the compositional distribution without simulation is discussed. Finally, conclusions are given.

METHODOLOGY

Fast DWMC for Two-Component Aggregative Mixing.

Spatially homogeneous two-component aggregation processes can be described by the bivariate PBE which is an extension of Smoluchowski's equation for one-component aggregation[18]

$$\begin{aligned}\frac{\partial n(m_A,\,m_B,\,t)}{\partial t} = \frac{1}{2}\int_0^{m_A}\int_0^{m_B} &K(m_A - m'_A,\,m_B - m'_B;\,m'_A,\,m'_B)n\\ &(m_A - m'_A,\,m_B - m'_B,\,t)n(m'_A,\,m'_B,\,t)\\ &dm'_A\,dm'_B - n(m_A,\,m_B,\,t)\\ &\int_0^\infty\int_0^\infty K(m_A,\,m_B,\,m'_A,\,m'_B,\,t)n\\ &(m'_A,\,m'_B,\,t)\,dm'_A\,dm'_B\end{aligned} \tag{6}$$

Here $K(m_A,m_B;m'_A,m'_B)$ is the aggregation rate coefficient (kernel) between a particle (m_A,m_B) and another particle (m'_A,m'_B).

For the two-component Brownian aggregation process which is the focus of this paper, numerical solutions of eq 6 are required. Deterministic methods (e.g., the sectional method[19] and the method of moments[20]) are computationally very efficient. However, if more than two internal particle properties have to be described, these methods lead to too complicated mathematical equations.[21] In contrast, stochastic methods known as population balance-Monte Carlo (PBMC) methods, are capable of simulating a large number of internal variables in a straightforward manner. The differentially weighted Monte Carlo (DWMC) method accurately determines the distributions of the multivariate properties over their full spectrum by means of differentially weighted simulation particles,[15−17,22−24] whereas conventional MC methods are accurate only in those regions of the spectra with sufficient simulation particles.

In the differentially weighted Monte Carlo method, the weight of a simulation particle i, w_i, indicates that the simulation particle i represents w_i real particles having the same internal variables as i. In order to determine the aggregation rate between simulation particles having different weights, a probabilistic aggregation rule was developed,[23] leading to

dx.doi.org/10.1021/ie500316g | Ind. Eng. Chem. Res. 2014, 53, 6047−6055

Table 1. Normal Kernels and Weighted Majorant Kernels for Brownian Aggregation in the Continuum and Free Molecular Regimes[a]

	case	formulation
in free molecular regime	normal kernel[1]	${}^{\mathrm{fm}}K_{ij} = (\pi k_B T/2)^{1/2}(m_i^{-1} + m_j^{-1})^{1/2}(d_i + d_j)^2$
	weighted majorant kernel	${}^{\mathrm{fm}}\hat{K}_{ij}' = 2\sqrt{2}\left(\frac{3}{4\pi}\right)^{1/6}\left(\frac{6k_BT}{\rho_{\min}}\right)^{1/2} v_j^{1/6} w_j \left[1 + \left(\frac{v_{\max}}{v_j}\right)^{1/6} + \left(\frac{v_{\max}}{v_j}\right)^{2/3} + \left(\frac{v_{\min}}{v_j}\right)^{-1/2}\right]$
in continuum regime	normal kernel[1]	${}^{\mathrm{co}}K_{ij} = \frac{2k_BT}{3\mu}(v_i^{1/3} + v_j^{1/3})\left(\frac{1}{v_i^{1/3}} + \frac{1}{v_j^{1/3}}\right)$
	weighted majorant kernel	${}^{\mathrm{co}}\hat{K}_{ij}' = \frac{4k_BT}{3\mu} w_j \left[2 + \left(\frac{v_{\max}}{v_j}\right)^{1/3} + \left(\frac{v_{\min}}{v_j}\right)^{-1/3}\right]$

[a]Note that k_B is Boltzmann's constant; T is the temperature of the medium; μ is the viscosity of the medium. If the material density of component A (ρ_A) is different from that of component B (ρ_B), the free-molecular kernel is composition-dependent. $\rho_{\min} = \min\{\rho_A, \rho_B\}$. When $\rho_A = \rho_B$, the kernel is composition-independent. The Brownian aggregation kernel in the continuum regime is composition-independent in nature. The left superscripts "fm" and "co" indicate the Brownian aggregation kernel in the free molecular and continuum regime, respectively.

$$\text{if } w_i \neq w_j, \begin{cases} w_i^* = \max(w_i, w_j) - \min(w_i, w_j);\ v_i^*(d_i^*; m_i^*; m_{Ai}^*) \\ \quad = v_k(d_k; m_{mk}; m_{Ak})|_{w_k = \max(w_i, w_j)} \\ w_j^* = \min(w_i, w_j);\ v_j^* = v_i + v_j;\ m_j^* = m_i + m_j;\ m_{Aj}^* \\ \quad = m_{Ai} + m_{Aj};\ d_j^* = (6v_j^*/\pi)^{1/3} \end{cases}$$

$$\text{if } w_i = w_j, \begin{cases} w_i^* = w_i/2;\ v_i^* = v_i + v_j;\ m_i^* = m_i + m_j;\ m_{Ai}^* \\ \quad = m_{Ai} + m_{Aj};\ d_i^* = (6v_i^*/\pi)^{1/3} \\ w_j^* = w_j/2;\ v_j^* = v_i + v_j;\ m_j^* = m_i + m_j;\ m_{Aj}^* \\ \quad = m_{Ai} + m_{Aj};\ d_j^* = (6v_j^*/\pi)^{1/3} \end{cases} \tag{7}$$

where v_i (v_j), d_i (d_j), and m_i (m_j) represent the volume, diameter, and mass of particle i (particle j), and m_{Ai} (m_{Aj}) is the mass of component A in particle i (particle j); k represents the new particle formed from the aggregation between two differentially weighted particles i and j; the asterisk indicates the value after the aggregation event. Equation 7 satisfies the law of mass conservation, and also keeps the number of simulation particles constant. On the basis of this rule, the aggregation rate of simulation particle i and j, the normalized kernel K_{ij}', is calculated as:[23]

$$K'_{ij} = \frac{2K_{ij} w_j \max(w_i, w_j)}{w_i + w_j} \tag{8}$$

Obviously K_{ij}' depends not only on the particle properties but also on the weights of the two simulation particles.

The conventional DWMC methods require double looping over all simulation particles so that the computational cost is as high as $O(N_{st}^2)$, where N_{st} is the total number of simulation particles. The smart bookkeeping technique, which updates the total aggregation rates of all simulation particles by correcting for the changed aggregation rates due to the changes induced by the selected aggregation pair, reduces these costs but still applies some form of local double looping.[23] In the paper we adopt the fast DWMC method to avoid the double looping.[25,26]

In the fast DWMC, the interacting particle pair is first selected using the acceptance-rejection (AR) method. Two randomly selected simulation particle i and j undergo an aggregation event if the following condition is met:

$$r \leq K'_{ij}/K'_{\max} \tag{9}$$

where r is a random number from an uniform distribution in the interval $[0, 1]$, $K'_{\max}$ is the maximum of the normalized aggregation kernel over all possible pairs. This procedure is repeated until a particle pair is accepted. It is worth noting that, even in the case that $K'_{\max}$ is overestimated, the acceptance–rejection method can still describe the Markov process exactly but less efficiently.

The AR process is effectively a random sampling process from the particle population, in which the average aggregation rate of all pairs of simulation particles, $\sum_{k=1}^{N_{AR}} K'_{ij,k}/N_{AR}$, will approximate the real average aggregation rate $\overline{K'_{ij}}$ of all possible pairs in the dispersed system when N_{AR} is not too small. Therefore, the time step in the fast-DWMC is approximated as

$$\Delta t = \frac{pVN_{st}}{\sum_{i=1}^{N_{st}} \sum_{j=1,\neq i}^{N_{st}} K'_{ij}} = \frac{pVN_{st}}{N_{st}(N_{st} - 1)\overline{K'}_{ij}} \approx \frac{pVN_{AR}}{(N_{st} - 1)\sum_{k=1}^{N_{AR}} K'_{ij,k}} \tag{10}$$

where $K'_{ij,k}$ is the normalized aggregation kernel for the kth particle pair in the AR selection process, N_{AR} is the number of particles pairs tested until acceptance, the empirical parameter p represents the ratio of the number of these particles selected for aggregation within one time step to N_{st}. In this paper, we put $p = 0.01$.[17] It is noted that in the fast DWMC method the sample size from the acceptance-rejection process, composed mainly of rejected pairs and some accepted pairs, should be at least 100 to ensure computational accuracy.

The key question of efficient PBMC modeling is how to approximate the maximum weighted kernel $K'_{\max}$ with minimal cost. The weighted majorant kernel is introduced to this purpose, based on the majorant kernel introduced by Wagner, Kraft and their co-workers.[27,28] The majorant kernel $\hat{K}_{ij}$ has the

dx.doi.org/10.1021/ie500316g | Ind. Eng. Chem. Res. 2014, 53, 6047−6055

Table 2. Conditions Used in Simulation Cases[a]

	N_{A0} (m^{-3})	d_{A0} (μm)	ρ_{A0} ($kg \cdot m^{-3}$)	ρ_{B0} ($kg \cdot m^{-3}$)	T (K)	μ (Pa·s)
case 1, in free-molecular regime	9×10^{21}	0.001	21.45×10^3	21.45×10^3	1800	5.65×10^{-5}
case 2, in free-molecular regime	9×10^{21}	0.001	7.87×10^3	21.45×10^3	1800	5.65×10^{-5}
case 3, in continuum regime	3×10^{15}	0.5	2.00×10^3	2.00×10^3	300	1.81×10^{-5}

[a]The volume of the computational domain, the number concentration ratio α, and particle diameter ratio β are varied in the simulations.

following characteristics: (1) $\hat{K}_{ij} \geq K_{ij}$ for all i, j; (2) $\hat{K}_{ij}$ can be formulated by $\hat{K}_{ij} = \sum_k[h_k(i) \times g_k(j)]$, where $h_k(i)$ is only dependent on particle i while $g_k(j)$ depends only on j; (3) $K_{ij}/\hat{K}_{ij}$ is close to 1. In the fast DWMC we utilize the characteristics of the majorant kernel to estimate K'_{max} through only single looping over all simulation particles. Knowing $(((2w_j\max(w_i,w_j))/(w_i + w_j)) \leq 2w_j)$, then $K'_{ij} = K_{ij}((2w_j\max(w_i, w_j))/(w_i + w_j)) \leq \hat{K}_{ij}((2w_j\max(w_i, w_j))/(w_i + w_j)) \leq 2\hat{K}_{ij}w_j = 2\sum_k[h_k(i) \times g'_k(j)] \leq 2\sum_k[\max(h_k(i)) \times g'_k(j)]$, where $g'_k(j) = g_k(j)w_j$. Therefore, we can define the weighted majorant kernel as follows

$$\hat{K}'_{ij} = 2\sum_k [\max(h_k(i)) \times g'_k(j)] \tag{11}$$

Through a single looping over all simulation particles, we can obtain $\max(h_k(i))$ in advance. Then $\hat{K}'_{ij}$ is only related to internal variables of one simulation particle (rather than particle pairs), i.e., $\hat{K}'_{ij} = \sum_k[f_k(j)]$, so that only the second single looping over all simulation particles is enough to estimate the maximum value over all $\hat{K}'_{ij}$, which is used to approximate $\hat{K}'_{max}$. Table 1 summarizes two typical Brownian aggregation kernels in different regimes and their weighted majorant kernels.

Even when the number of simulation particles can be kept constant throughout the simulation, the MC method still leads to a great deal of statistical noise in the distribution functions when there is an insufficient number of simulation particles in a specific region of the internal variables. This makes it impossible to determine the compositional distributions in this region. In order to determine accurately the distributions of internal variables over their full spectrum, a finite number of simulation particles has to be distributed homogeneously over the multidimensional joint space of internal variables, rather than letting them evolve freely. When certain conditions are reached, for example, when the number concentration of real particles is halved, a shift action is performed which restricts the number of simulation particles in predefined size and composition intervals. This action increases the simulation particle number in less-populated regions by splitting some simulation particles in less-populated regions into more simulation particles and decreases the simulation particle number in densely populated regions by randomly removing some simulation particles in densely populated regions from the simulation. Its implementation has been described already.[15,17]

Validation. Two reference cases with composition-independent/dependent Brownian kernels in the free-molecular regime described in ref 15 are used for validating the fast DWMC method through comparison with the conventional DWMC method. The simulation conditions for the two cases (together with other cases which will be shown also in this paper) are summarized in Table 2.

For the composition-independent case, a two-component particle population having the same density (21.45×10^3 kg m^{-3}, the metal Pt) but different initial diameters and number concentrations is selected (case 1). At $t = 0$, when putting $N_{A0} = 9N_{B0}$, $d_{A0} = d_{B0}/2 = 1$ nm, the mass fraction of component A is $\phi = 0.5294$ and $\chi_0 = 1.3167 \times 10^{-23}$ so that $\chi_0/m_{A0} = 1.1724$. The composition-dependent case is identical, except that $\rho_A \neq \rho_B$. In this case $\phi = 0.2922$, $\chi_0 = 6.0321 \times 10^{-24}$, and $\chi_0/m_{A0} = 1.4638$.

The simulation starts with 10 000 simulation particles and limits the simulation particle number to 30 000. The MC simulations are repeated five times using different seeds for the random number generator. Figure 1 shows the mass-normalized power density of excess component A (χ) and segregation index ($\chi/\bar{m}$) as function of dimensionless time for aggregative mixing (cases 1 and 2): comparison between the conventional DWMC method and the fast DWMC.

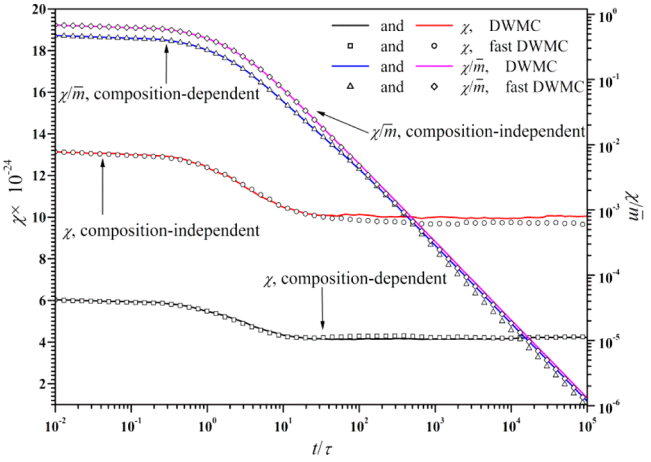

Figure 1. Mass-normalized power density of excess component A (χ) and segregation index ($\chi/\bar{m}$) as function of dimensionless time for aggregative mixing (cases 1 and 2): comparison between the conventional DWMC method and the fast DWMC.

normalized power density of excess component A (χ) and segregation index ($\chi/\bar{m}$, where $\bar{m}$ is the mean particle mass) against time made dimensionless with the characteristic aggregation time scale, τ, which is defined as $1/(2\bar{K}_0N_0)$ for an initially bidisperse distribution, where N_0 is the initial total number concentration and $\bar{K}_0$ is the initial mean kernel over all possible particle pairs. It is clear from comparison with the benchmark DWMC method that, in spite of the approximations adopted in the fast DWMC, its computational accuracy is sufficiently high. As expected, the fast DWMC method accelerates the PBM considerably, achieving a speedup ratio of more than 100. In a desktop PC equipped with a Intel(R) Core(TM)2 Quad Q9300 CPU (2.5 GHz, 3.5 GB RAM), the conventional DWMC takes 7131 s for case 1, compared to only 68 s using the fast DWMC.

RESULTS

Screening the Relevant Parameters for χ_∞/χ_0. The steady-state value of χ (χ_∞) is usually of the same order as its initial value, as can be seen from Figure 1. One can thus speculate that the degree of mixing between components, which is controlled by χ (cf. eq 3), is largely controlled by the initial degree of mixing. Introducing the following ratios

dx.doi.org/10.1021/ie500316g | Ind. Eng. Chem. Res. 2014, 53, 6047−6055

$$\alpha = \frac{N_{A0}}{N_{B0}}, \quad \beta = \frac{d_{A0}}{d_{B0}}, \quad \gamma = \frac{\rho_A}{\rho_B} \tag{12}$$

and defining the overall number fraction of component A

$$\varphi = \frac{N_{A0}}{N_{A0} + N_{B0}} = \frac{\alpha}{1 + \alpha} \tag{13}$$

and calculating the overall mass fraction of component A

$$\phi = \frac{M_{A0}}{M_{A0} + M_{B0}} = \frac{\alpha\beta^3\gamma}{1 + \alpha\beta^3\gamma} \tag{14}$$

it is possible to calculate the initial degree of mixing χ_0 in the bidisperse case as[13,14]

$$\begin{aligned}\chi_0 &= (1 - \phi)\phi(m_{A0}(1 - \phi) + m_{B0}\phi) \\ &= \frac{\alpha\beta^3\gamma(1 + \alpha)}{(1 + \alpha\beta^3\gamma)^3} m_{A0} \\ &= \frac{\phi(1 - \phi)^2}{(1 - \varphi)} m_{A0}\end{aligned} \tag{15}$$

It is postulated that χ_∞/χ_0 depends only on the initial feeding condition and parameters associated with the Brownian aggregation kernel, so that χ_∞/χ_0 may be related to the following parameters: T, N_{A0}, d_{A0}, ρ_A, α, β, and γ. These influencing factors are now one by one examined.

For this analysis, the composition-dependent case (case 2) is applied: we first fix the other parameters and change the temperature T. In this way, the influence of T on χ_∞/χ_0 is examined. As shown in Figure 2, using different T (1800, 2700, and 3600 K) while keeping the other parameters constant, does not influence χ/χ_0. Similarly, it is found that N_{A0}, d_{A0}, and ρ_A are noninfluencing parameters for χ_∞/χ_0 as long as the parameters α, β, and γ are kept constant, as shown exemplary also for N_{A0} in Figure 2. The independence of the time evolution of the degree of mixing from the values of T, N_{A0}, d_{A0}, and ρ_A is due to the dimensionless representation of the results in Figure 2, e.g., the increased number concentration will lead to larger value of the characteristic aggregation time scale, τ. However, α, β, and γ are the relevant parameters determining χ_∞/χ_0 because changing them leads to different χ_∞/χ_0, as will be shown below. It is thus concluded that χ_∞/χ_0 is a function of three parameters α, β, and γ. We further explore their relation. Once two parameters, for example, α and γ, are fixed, a deterministic relation between χ_∞/χ_0 and the remaining parameter (e.g., β) can be obtained by fitting the PBMC simulation results.

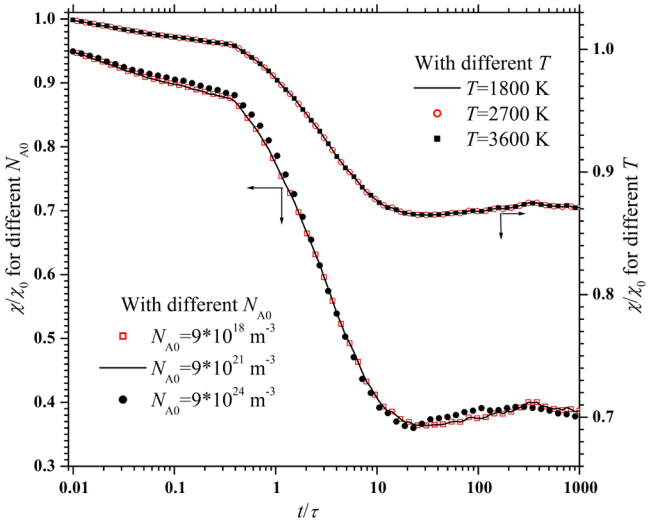

Figure 2. χ_∞/χ_0 as function of the dimensionless time: one-factor-at-a-time testing of N_{A0} (left axis) and T (right axis).

χ_∞/χ_0 as Function of α and β: Composition-Independent Case (γ = 1) in the Free Molecular Regime. With respect to composition-independent Brownian aggregation in the free molecular regime (i.e., $\rho_A = \rho_B$, so that $\gamma = 1$), we vary systematically the relevant parameters to obtain the relation between χ_∞/χ_0 and ϕ.

With regard to initially bidisperse distribution, the initial χ can be rewritten as follows:[13]

$$\begin{aligned}\chi_0 &= \frac{\bar{m}_0(1 - \phi)\phi[(1 - \beta^3\gamma)\phi + \beta^3\gamma]^2}{\beta^3\gamma} \\ &= \frac{\bar{m}_0(1 - \phi)^2\phi^2(1 + \alpha)^2}{\alpha}\end{aligned} \tag{16}$$

where the initially mean particle mass $\bar{m}_0 = m_{A0}/[\beta^3\gamma + \phi(1 - \beta^3\gamma)] = m_{A0}\alpha/[\phi(1 + \alpha)]$. Lee et al. found that the minimal initial degree of mixedness for a given ϕ is obtained when α = 1.[13] The minimal $\chi_0/\bar{m}_0$ is therefore

$$(\chi_0/\bar{m}_0)_{min} = 4\phi^2(1 - \phi)^2 \tag{17}$$

However, the relation of χ_∞ and χ_0 is still not known for the case α = 1. When γ = 1 and α = 1, χ_∞/χ_0 is a function of ϕ. We use the simulation results of the fast DWMC method to fit the function $\chi_\infty/\chi_0 = f(\phi)$. χ_∞/χ_0 is fitted as a function of ϕ(equivalent to varying β) to the following Gaussian function, as shown in Figure 3

$$\frac{\chi_\infty}{\chi_0} = C_1 \exp\left[-2\left(\frac{\phi - \phi_{\beta=1}}{C_2}\right)^2\right] \tag{18}$$

where the values of the fitting constants C_1 and C_2 are shown in Table 3 and $\phi_{\beta=1} = \alpha/(\alpha + 1)$ is the value of φ where χ_∞/χ_0 is at its maximum.

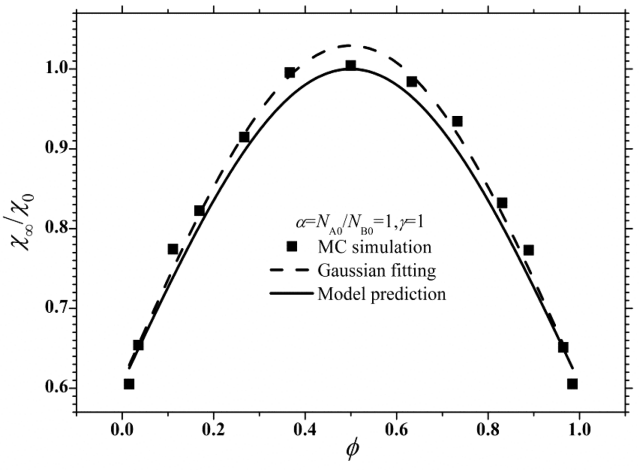

Figure 3. χ_∞/χ_0 as a function of ϕ: γ = 1 and α = 1 in the free molecular regime. The Gaussian best fit is obtained with eq 18, and the model prediction is according to eq 19.

dx.doi.org/10.1021/ie500316g | Ind. Eng. Chem. Res. 2014, 53, 6047−6055

Table 3. Constants C_1 and C_2 Obtained from Fitting eq 20 to Simulation Results from the MC Simulations

α	C_1	C_2
1	1.02935	0.97646
10	1.00886	0.99963
2	0.99735	1.09858
0.1	1.00632	0.97545
0.5	1.00104	1.04163

For an initially monodisperse distribution ($\beta = 1$), Matsoukas et al. found that χ is not dependent on the initial number concentration ratio α.[12,13] Our simulation results shown in Figure 4 indeed show that the variation in ϕ, obtained by varying α, does not change χ_∞/χ_0 significantly.

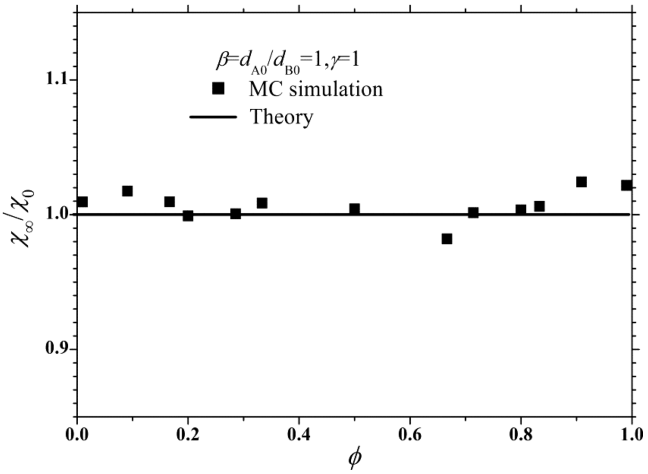

Figure 4. χ_∞/χ_0 independent of ϕ when $\gamma = 1$ and $\beta = 1$ in the free molecular regime.

Four more cases with different values of α are simulated and fitted to eq 18. The resulting constants C_1 and C_2 are shown in Table 3.

From Table 3, it can be seen that the constants C_1 and C_2 are close to 1. Therefore, χ_∞/χ_0 as a function of ϕ can be effectively approximated as

$$\frac{\chi_\infty}{\chi_0} = \exp[-2(\phi - \phi_{\beta=1})^2] \tag{19}$$

so that it can be concluded that the main parameters determining χ_∞/χ_0 are the overall mass fraction of component A, ϕ, and initial number ratio $\varphi = \phi_{\beta=1}$ when $\gamma = 1$. The predictions from eq 19 are also shown in Figures 3 and 4. It is found that this general model does describe the DWMC simulation results quite well. We also examine whether the general Gaussian statistics eq 19 is valid for more general cases (case 1 in Table 1) when varying both ϕ and φ. We simulate 19 × 19 cases, where ϕ and φ are given a value among {0.05, 0.1, 0.15, 0.2, ..., 0.90, 0.95}, respectively. We present the simulation results and the model prediction from eq 19 in Figure 5, including the standard deviations for the 361 cases (obtained by repeating each simulations 5 times). In view of the inherent statistical noise of MC simulations, the relation between χ_∞/χ_0 and the initial feed conditions is reasonably described by eq 19 for composition-independent aggregative mixing ($\gamma = 1$).

χ_∞/χ_0 is also shown as contour plot as a function of ϕ and φ in Figure 6. It appears that there is a slight dependency on both

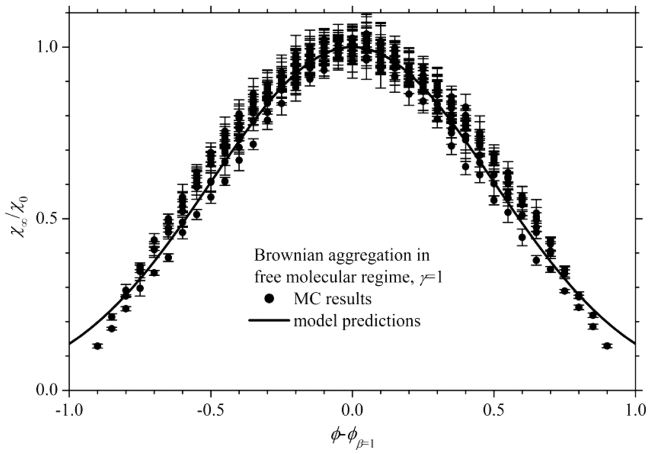

Figure 5. Comparison between of eq 19 and MC simulations of χ_∞/χ_0 as a function of $\phi - \phi_{\beta=1}$ for 361 different combinations of ϕ and φ ($\gamma = 1$, free molecular regime).

ϕ and φ, which is not present in eq 19 as it shows only a dependency on $\phi - \varphi$.

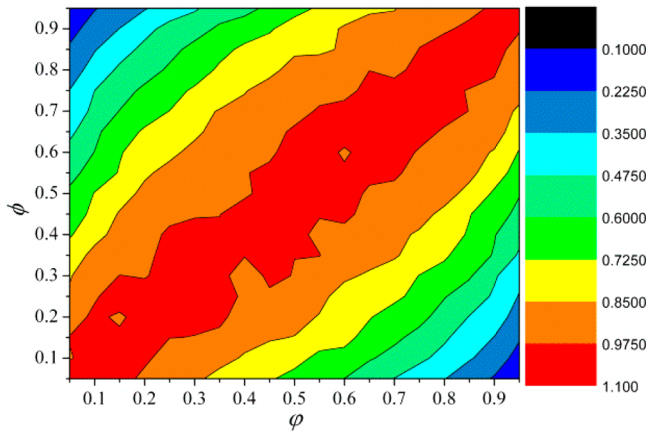

Figure 6. Contour plot of χ_∞/χ_0 as a function of ϕ and $\varphi = \phi_{\beta=1}$ ($\gamma = 1$, free molecular regime).

χ_∞/χ_0 as Functions of α and β: Composition-Dependent Case in the Free Molecular Regime ($\gamma \neq 1$). The suitability of eq 19 for describing composition-dependent aggregative mixing ($\gamma \neq 1$) is investigated as well. Aggregative mixing of Fe/Pt nanoparticles is taken as example (case 2 in Table 2). Now the composition-dependent kernel in the free molecular regime is a function of the sizes of two interacted particles and their densities, and $\phi_{\beta=1} = \alpha\gamma/(\alpha\gamma + 1)$. We simulate again 19 × 19 cases similar to the component-independent aggregation in the above section, the results are shown in Figure 7. The Gaussian approximation from eq 19 seems to be able to predict χ_∞/χ_0 reasonably, although with decreasing reliability at the right part of the curve. The curve seems to indicate that the component density ratio is not so relevant for the estimation of χ_∞/χ_0.

χ_∞/χ_0 as Functions of α and β: in the Continuum Regime. In order to explore the dependency of χ_∞/χ_0 on the aggregation kernel the same study is performed now using the kernel for the continuum regime. It is noted that this Brownian aggregation kernel is composition-independent in nature since it is related to the particle size (volume) rather than the particle mass. The fast DWMC is used to simulate 19 × 19 cases (case

dx.doi.org/10.1021/ie500316g | Ind. Eng. Chem. Res. 2014, 53, 6047−6055

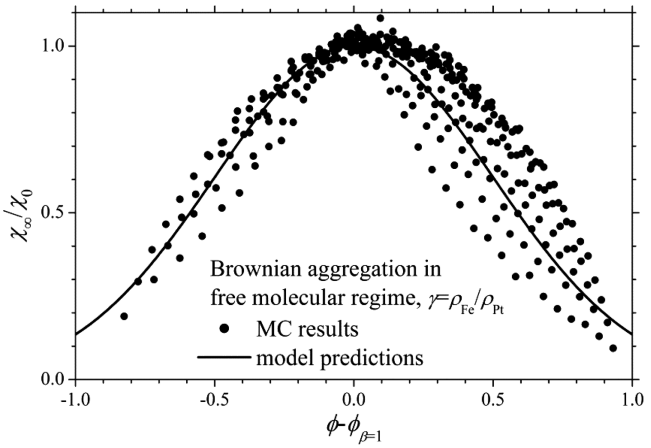

Figure 7. χ_∞/χ_0 as a function of $\phi - \phi_{\beta=1}$ in the free molecular regime: $\gamma = \rho_{Fe}/\rho_{Pt}$.

3 in Table 2) to explore the relation between χ_∞/χ_0 and the feeding conditions. Again, χ_∞/χ_0 as a function of $\phi - \phi_{\beta=1}$ satisfies the Gaussian function, however with a different geometric standard deviation, as expressed in eq 20 and shown in Figure 8

$$\frac{\chi_\infty}{\chi_0} = \exp\left[\frac{-(\phi - \phi_{\beta=1})^2}{\sqrt{2}}\right] \quad (20)$$

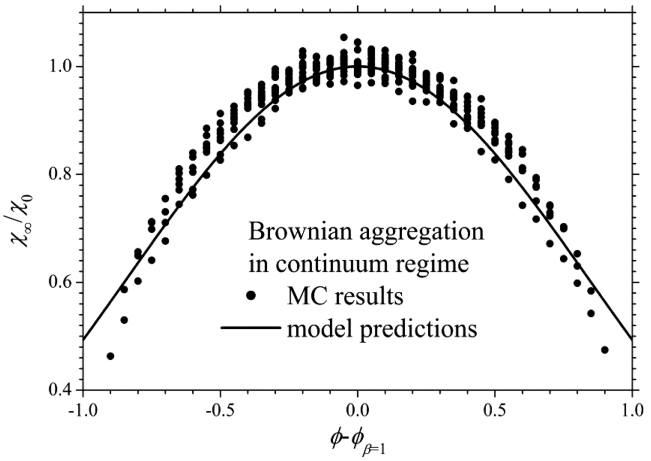

Figure 8. χ_∞/χ_0 as a function of $\phi - \phi_{\beta=1}$ in the continuum regime. The model predictions refer to eq 20.

DISCUSSION

In order to examine the validity of the general formulas predicting χ_∞/χ_0, we compare the predictions from eqs 19 and 20 with published data. We have selected simulation cases with initial bidisperse distribution and the aggregation kernel obtained from the kinetic theory of granular flow, which has an identical size dependency as the aggregation kernel in the free-molecular regime. As presented in Figure 7 in the work of Lee et al.,[13] the χ at the mean granule size of 1 is considered to be the initial value χ_0, while the χ at the mean granule size of 10^5 obtained by their constant-number Monte Carlo simulation is considered to be the steady-state value χ_∞. For $\phi = 0.1$, $\beta^3 = 1/10$ and $\gamma = 1$, the ratio of the steady-state χ_∞ and χ_0 is 0.6953 according to eq 19, while the constant-Number simulation yielded 0.6603 as estimated from the figure.[13] For the case of $\phi = 0.5$, $\beta^3 = 1/10$ and $\gamma = 1$, $\chi_\infty/\chi_0 = 0.7156$ from eq 19 and 0.6695 from the MC simulation. It is obvious that the final degree of mixing predicted by eq 19 agrees well with the results from the constant-number Monte Carlo simulation. The deviation between the MC results and the formula predictions is less than 6.5% for both cases. This deviation is fully acceptable, considering that a single constant-number MC simulation shows fluctuations of about ±5% from the mean value.

With the proposed formulas, we can predict the compositional distributions at any time and for any size fraction without complex and time-consuming simulations, when knowing the initial feeding conditions. For example, we use the formula and the PBMC simulation to attain the A-component distributions within selected intervals for Case 1 with the initial number concentration ratio (α) of 9 and the initial particle diameter ratio (β) of 0.5 and the composition density ratio (γ) of 0.3669. The corresponding PBMC simulation results have been presented in earlier work.[15] The theoretical predictions of the compositional distributions with selected size intervals can be calculated by combining eq 5 and eq 19 (in the free-molecular regime) or eq 20 (in the continuum regime). Figure 9 shows

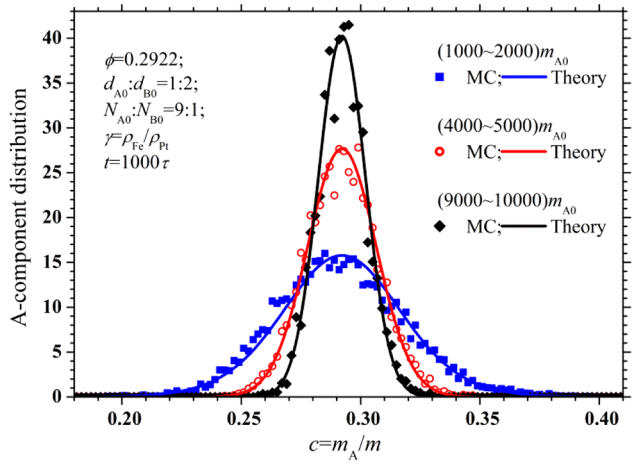

Figure 9. Compositional distributions within selected intervals: comparison between the formula predictions and the PBMC simulations.

the compositional distributions at three size intervals (mass interval $(1000-2000)m_{A0}$, $(4000-5000)m_{A0}$, $(9000-10000)m_{A0}$) when $t = 1000\tau$. The figure shows a very good agreement between the theoretical predictions and the PBMC simulation results.

The formulas explored in this paper have a practical relevance for processing of solid-state particulate materials in an industrial environment. For example, in pharmaceutical granulation where an active pharmaceutical ingredient is cogranulated with an inert excipient to prepare functional tablets with specified size and composition, it is necessary to control the size distribution as well the compositional distribution of the components among granules of different sizes. It is possible to control the size distribution by adjusting the granulation reactor and on the other hand, to control the compositional distribution by selecting the initial feeding parameters, or to achieve an optimal operation for both the size and compositional distributions.

dx.doi.org/10.1021/ie500316g | Ind. Eng. Chem. Res. 2014, 53, 6047−6055

It is noted that the explored Gaussian-type formulas for the ratio of the steady-state value of χ (χ_∞) and its initial value χ_0 as function of the initial feeding conditions may be limited by the following assumptions. (1) Brownian aggregation either in the free-molecular or the continuum regime. As for Brownian aggregation occurs often in the transition regime, a possible approach could be to apply the harmonic mean kernel (i.e., ${}^{\mathrm{tr}}K_{ij} = ((1/{}^{\mathrm{co}}K_{ij}) + (1/{}^{\mathrm{fm}}K_{ij}))^{-1}$). It has to be investigated whether the Gaussian function (eq 19) available for the free molecular regime is also able to formulate the relation between χ_∞/χ_0 and $\phi - \phi_{\beta=1}$ for the aggregation kernel in the transition regime. (2) Throughout two-component aggregative mixing, those external parameters which influence the aggregation rate, such as the reactor temperature and the medium viscosity, should be kept constant. (3) The two components do not react chemically. (4) The aggregative mixing starts from primary particles containing either component A or component B. (5) The aggregates are assumed to have a spherical shape, so that a possible fractal structure is not considered. (6) Other dynamic events such as breakage, condensation/evaporation, nucleation, and settlement are not considered. However, if the breakage rate is far smaller than the aggregation rate and chemical reactions do not occur, conditions often encountered in, e.g., high-temperature synthesis of alloyed nanoparticles and pharmaceutical granulation, the Gaussian functions should be valid. Otherwise, population balance modeling describing all of the relevant mechanisms should be carried out to predict the size and compositional distributions in these more complicated systems.

CONCLUSIONS

Two-component aggregative mixing is strongly dependent on the initial mixture state of the components, e.g., the ratio of the particle volume of the two components at the start of the aggregation process. With respect to two-component aggregative mixing due to Brownian coagulation with initially bidisperse distributions, theory predicts and simulations confirmed that compositional distributions can be characterized by a Gaussian function once the self-preserving distribution is formed at large times. This Gaussian-type compositional distribution is determined by the overall mass fraction of component A (ϕ, which is known in advance once the feeding condition is given) and the mass-normalized power density of excess component A (χ). Investigations showed that χ always reaches a steady-state value for bicomponent aggregation. In this work, we found that it is possible to predict the ratio of the steady-state value of χ (χ_∞) and its initial value χ_0 as function of the initial feeding conditions, based on bivariate population balance modeling using a Monte Carlo method. In order to be able to simulate the large number of simulation cases necessary for the parameter studies, a fast version of the differentially weighted Monte Carlo method with the compositional-dependent shift action has been implemented. The simulations showed that the ratio χ_∞/χ_0 depends on three parameters, that is, the initial number ratio α ($=N_{A0}/N_{B0}$), the initial diameter ratio β ($=d_{A0}/d_{B0}$), and the component density ratio γ ($=\rho_A/\rho_B$). Based on preliminary analysis and model fitting from hundreds of simulations, a good estimation of χ_∞/χ_0 as function of ϕ is given by the following Gaussian-type function: $\chi_\infty/\chi_0 = \exp[-2(\phi - \phi_{\beta=1})^2]$ for Brownian aggregation in the free molecular regime and $\chi_\infty/\chi_0 = \exp[-(\phi - \phi_{\beta=1})^2/\sqrt{2}]$ in the continuum regime. The proposed Gaussian-type functions would benefit from experimental investigation of the composition of sufficiently large numbers of individual particles formed by bicomponent aggregation, which is however rather time-consuming and costly.

AUTHOR INFORMATION

Corresponding Author

*Tel.: +86-27-8754-4779. Fax: +86-27-8754-5526. E-mail: klinsmannzhb@163.com.

Notes

The authors declare no competing financial interest.

ACKNOWLEDGMENTS

H.Z. was supported with funds from "The National Natural Science Foundation of China" (51276077 and 51390494) and "National Key Basic Research and Development Program"(2010CB227004). F.E.K. was supported by the Priority Program SPP 1679 "Dynamic Simulation of coupled solid-state processes" of the Deutsche Forschungsgemeinschaft (DFG).

REFERENCES

(1) Friedlander, S. K. *Smoke, Dust and Haze: Fundamentals of Aerosol Dynamics*, 2nd ed.; Oxford University Press: New York, 2000.

(2) Singh, J.; Patterson, R. I. A.; Kraft, M.; Wang, H. Numerical Simulation and Sensitivity Analysis of Detailed Soot Particle Size Distribution in Laminar Premixed Ethylene Flames. *Combust. Flame* **2006**, *145*, 117−127.

(3) DeVille, R. E. L.; Riemer, N.; West, M. Weighted Flow Algorithms (WFA) for Stochastic Particle Coagulation. *J. Comput. Phy.* **2011**, *230*, 8427−8451.

(4) Hosseini, A.; Bouaswaig, A.; Engell, S. Novel Approaches to Improve the Particle Size Distribution Prediction of a Classical Emulsion Polymerization Model. *Chem. Eng. Sci.* **2013**, *88*, 108−120.

(5) Barrasso, D.; Ramachandran, R. A Comparison of Model Order Reduction Techniques for a Four-Dimensional Population Balance Model Describing Multi-component Wet Granulation Processes. *Chem. Eng. Sci.* **2013**, *80*, 380−392.

(6) Hofmann, S.; Raisch, J. Solutions to Inversion Problems in Preferential Crystallization of Enantiomers-Part II: Batch Crystallization in Two Coupled Vessels. *Chem. Eng. Sci.* **2013**, *88*, 48−68.

(7) Riemer, N.; West, M.; Zaveri, R.; Easter, R. Estimating Black Carbon Aging Time-Scales With a Particle-Resolved Aerosol Model. *J. Aerosol Sci.* **2010**, *41*, 143−158.

(8) West, R. H.; Shirley, R. A.; Kraft, M.; Goldsmith, C. F.; Green, W. H. A Detailed Kinetic Model for Combustion Synthesis of Titania from $TiCl_4$. *Combust. Flame* **2009**, *156*, 1764−1770.

(9) Lin, J. J.; Loh, L. S.; Lee, P.; Tan, T. L.; Springham, S. V.; Rawat, R. S. Effects of Target-Substrate Geometry and Ambient Gas Pressure on FePt Nanoparticles Synthesized by Pulsed Laser Deposition. *Appl. Surf. Sci.* **2009**, *255*, 4372−4377.

(10) Krapivsky, P. L.; Ben-Naim, E. Aggregation With Multiple Conservation Laws. *Phys. Rev. E* **1996**, *53*, 291−298.

(11) Vigil, R. D.; Ziff, R. M. On the Scaling Theory of Two-Component Aggregation. *Chem. Eng. Sci.* **1998**, *53*, 1725−1729.

(12) Matsoukas, T.; Lee, K.; Kim, T. Mixing of Components in Two-Component Aggregation. *AIChE J.* **2006**, *52*, 3088−3099.

(13) Lee, K.; Kim, T.; Rajniak, P.; Matsoukas, T. Compositional Distributions in Multicomponent Aggregation. *Chem. Eng. Sci.* **2008**, *63*, 1293−1303.

(14) Matsoukas, T.; Kim, T.; Lee, K. Bicomponent Aggregation with Composition-Dependent Rates and the Approach to Well-mixed State. *Chem. Eng. Sci.* **2009**, *64*, 787−799.

(15) Zhao, H.; Kruis, F. E.; Zheng, C. Monte Carlo Simulation for Aggregative Mixing of Nanoparticles in Two-Component Systems. *Ind. Eng. Chem. Res.* **2011**, *50*, 10652−10664.

(16) Zhao, H.; Zheng, C. Two-Component Brownian Coagulation: Monte Carlo Simulation and Process Characterization. *Particuology* **2011**, *9*, 414−423.
(17) Zhao, H.; Kruis, F. E.; Zheng, C. A Differentially Weighted Monte Carlo Method for Two-Component Coagulation. *J. Comput. Phys.* **2010**, *229*, 6931−6945.
(18) Lushnikov, A. A. Evolution of Coagulating Systems: III. Coagulating Mixtures. *J. Colloid Interface Sci.* **1976**, *54*, 94−101.
(19) Chauhan, S. S.; Chakraborty, J.; Kumar, S. On the Solution and Applicability of Bivariate Population Balance Equations for Mixing in Particle Phase. *Chem. Eng. Sci.* **2010**, *65*, 3914−3927.
(20) Fox, R. O. Higher-Order Quadrature-Based Moment Methods for Kinetic Equations. *J. Comput. Phys.* **2009**, *228*, 7771−7791.
(21) Marshall, C. L., Jr; Rajniak, P.; Matsoukas, T. Numerical Simulations of Two-Component Granulation: Comparison of Three Methods. *Chem. Eng. Res. Des.* **2010**, *89*, 545−552.
(22) Zhao, H.; Zheng, C. A New Event-driven Constant-Volume Method for Solution of the Time Evolution of Particle Size Distribution. *J. Comput. Phys.* **2009**, *228*, 1412−1428.
(23) Zhao, H.; Kruis, F. E.; Zheng, C. Reducing Statistical Noise and Extending the Size Spectrum by Applying Weighted Simulation Particles in Monte Carlo Simulation of Coagulation. *Aerosol Sci. Technol.* **2009**, *43*, 781−793.
(24) Zhao, H.; Zheng, C. A Population Balance-Monte Carlo Method for Particle Coagulation in Spatially Inhomogeneous Systems. *Comput. Fluids* **2013**, *71*, 196−207.
(25) Hao, X.; Zhao, H.; Xu, Z.; Zheng, C. Population Balance-Monte Carlo Simulation for Gas-to-Particle Synthesis of Nanoparticles. *Aerosol Sci. Technol.* **2013**, *47*, 1125−1133.
(26) Xu, Z.; Zhao, H.; Zheng, C. Fast Monte Carlo Simulation for Particle Coagulation in Population Balance. *J. Aerosol Sci.*, in press.
(27) Eibeck, A.; Wagner, W. Approximative Solution of the Coagulation-Fragmentation Equation by Stochastic Particle Systems. *Stoch. Anal. Appl.* **2000**, *18*, 921−948.
(28) Goodson, M.; Kraft, M. An Efficient Stochastic Algorithm for Simulating Nano-particle Dynamics. *J. Comput. Phys.* **2002**, *183*, 210−232.